

# IBM Research Report

## Study of Oxidation of Sn-Pb Solders for Microelectronic Applications

**Sung-il Cho, Jin Yu**

Department of Materials Science and Engineering  
Korea Advanced Institute of Science and Technology (KAIST)  
373-1 Kusung-dong, Yusung, Daejeon 305-701, Korea

**Sung K. Kang, Da-Yuan Shih**

IBM Research Division  
Thomas J. Watson Research Center  
P.O. Box 218  
Yorktown Heights, NY 10598



Research Division

Almaden - Austin - Beijing - Haifa - India - T. J. Watson - Tokyo - Zurich

# Study of Oxidation of Sn-Pb Solders for Microelectronic Applications

Sung-il Cho, Jin Yu,  
*Department of Materials Science and Engineering*  
*Korea Advanced Institute of Science and Technology (KAIST)*  
*373-1 Kusung-dong, Yuseong, Daejeon 305-701, Korea*

Sung K. Kang, Da-Yuan Shih  
*IBM T. J. Watson Research Center, Yorktown Heights, NY 10598*

## ABSTRACT

The oxidation of pure Sn and eutectic 63Sn-37Pb solder was investigated at 85°C in either dry air or a humid environment at 85% relative humidity (R.H.). Both the chemical nature of oxide and its thickness were characterized using the Sequential Electrochemical Reduction Analysis (SERA) technique by measuring the electrolytic reduction potential and total transferred electrical charges for each alloy composition and oxidizing condition. For pure Sn, SnO is shown to grow faster under humid condition than in dry air, while a very thin (<10 Å) layer of SnO<sub>2</sub> is always formed on the top surface of both alloys. For eutectic 63Sn-37Pb, a mixture layer of SnO and SnO<sub>2</sub> is formed and SnO<sub>2</sub> is shown to grow thick when aged under the humid condition.

Most metal tends to form surface oxides spontaneously under ambient or aqueous condition<sup>1,2</sup>. The presence of oxides on the surface of solder alloys used in microelectronics applications is of critical importance. It affects the formation of otherwise a good solder joint by degrading their wettability and solderability<sup>3, 4</sup>. In manufacturing, a flux material is typically used to reduce surface oxides and to prevent the joining surfaces from further oxidation during reflow at elevated temperatures. However, the environmentally friendly flux materials used in microelectronics assembly such as no-clean flux and water-soluble flux do not warrant an oxide-free surface during soldering<sup>5</sup>.

Continued interaction of oxygen with solder during the service period of microelectronics products can affect the mechanical reliability of solder joints. It was reported that when a Pb-rich Sn solder is fatigued in air, the intergranular cracks dominate, while fatigued in a vacuum, the transgranular cracks dominate. The fatigue life is also shortened for the air-fatigued samples, suggesting that oxygen diffusion at grain boundaries plays an important role in the lifetime of solder joints<sup>6</sup>. Hence, it is important to characterize the oxidation behavior of solder joints during the soldering process as well as in service to better understand their reliability issues.

There are many techniques<sup>1</sup> to characterize the surface oxides. AES<sup>7</sup>, XPS<sup>8</sup>, LEELS<sup>9</sup> and Mössbauer<sup>10</sup> are for chemical information of oxides. Ellipsometry, X-ray emission, gravimetric method and AES are techniques to measure oxide thickness. None of these techniques provides complete information of the oxides. Electrochemical reduction analysis is known to be an inexpensive, simple and yet relatively precise technique to measure quantitatively both the type and the thickness of oxides formed on metal surfaces<sup>4</sup>. In this study, a SurfaceScan<sup>®</sup> QC-100 tool developed by ECI technology (East Rutherford, NJ) for sequential electrochemical reduction analysis (SERA) was used to study the oxidation of pure Sn and eutectic Sn-Pb solder alloys.

In the SERA method, the surface to be analyzed is brought in contact with an electrolyte, which is made of sodium borate and boric acid. A constant cathodic current is applied between the surface and an inert counter electrode<sup>4</sup>. The change of cathode potential of the oxidized surface during reduction is recorded as a function of time relative to a reference electrode. The recorded potential-time curve consists of a series of potential durations (plateaus), which is characteristic of each type of oxides reduced. The equilibrium reduction potentials for Sn and Pb oxides are shown in Table 1. After completing the reduction process, the final plateau of hydrogen evolution begins due to reduction of the electrolyte. In this study electrochemical

reduction was performed at  $20\mu\text{A}/\text{cm}^2$  using Ag/AgCl as reference electrode (+0.2224 vs. SHE)<sup>11</sup> in a nitrogen-saturated borate buffer solution of pH 8.4 which provides a minimal solubility for tin oxides<sup>12</sup>. Table 1 shows the Gibbs free energy<sup>13, 14</sup>,  $\Delta G^\circ$ , of each oxide and equilibrium reduction values calculated from the Nernst equation<sup>2</sup> using  $\Delta G^\circ$  values according to the reaction typified by:

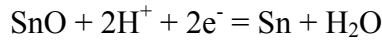


Figure 1 shows the SERA curves for pure oxide powders of Sn and Pb and they were used as a standard to calibrate and distinguish different types of oxides in this study. The measured reduction potentials of each oxide are listed in Table 1 to compare with the equilibrium values. Because of kinetic factors, actual reduction potentials are generally more negative than theoretical values in agreement with the previous observation<sup>4</sup>. Although the equilibrium potential of SnO<sub>2</sub> is almost the same as SnO, the measured potential for SnO<sub>2</sub> is somewhat lower than that of SnO, indicating that the reduction of SnO<sub>2</sub> is kinetically somewhat inhibited. The reduction potential of a mixture of SnO and SnO<sub>2</sub> powders exhibits a decreasing intermediate value between SnO and SnO<sub>2</sub>. The reduction of SnO continues as the potential decreases to the level of reduction for SnO<sub>2</sub> and then SnO<sub>2</sub> reduces solely. The decreasing reduction potential of SnO was also observed with pure Sn and eutectic 63Sn-37Pb as discussed below. 99.99% pure Sn and eutectic 63Sn-37Pb cast ribbons were thermally oxidized at 85°C in dry air and under a humid condition (85% RH), respectively. The surface of the ribbon samples was fully reduced electrochemically using the same electrolyte used for SERA but at a high current density before placed in an oxidizing chamber.

Figure 3 and 4 show the SERA reduction curves of pure Sn oxidized at 85°C in dry air as well as under a temperature (85°C) and humidity condition (85% R.H.) up to 10 days, respectively. The native oxide of pure Sn formed in air right after reduction (i.e., as-reduced) was SnO and the thickness was about 10Å. The thickness of oxide was calculated using the modified Faraday's equation<sup>15</sup> where the time required to reduce surface oxide is directly proportional to the thickness of an oxide and the oxide is assumed in the form of a uniform layer:

$$T = (\text{Mit}) / (\text{nFSD})$$

where  $M$ =Molecular weight,  $i$ =current,  $t$ =time,  $n$ =number of electrons,  $F$ =Faraday's constant,  $D$ =density of coating,  $S$ =surface area.

Figure 2 and 3 show the growth of SnO on pure Sn surface with the reduction potential of  $-0.8$  V, which is close to the equilibrium value. SnO grows faster under the humid condition than in dry air. A small negative peak at the initial stage of reduction is thought to be the reduction of a very thin SnO<sub>2</sub> overlayer<sup>4, 11</sup>. Since SnO reduces first at a more positive potential with respect to SnO<sub>2</sub>, the initial peak indicates that SnO<sub>2</sub> exists in the form of an overlayer preventing the exposure of SnO to the electrolyte. As shown in Figure 3, the small negative peak around the reduction potential of SnO<sub>2</sub> increases in thickness as the oxidation time increases under the T/H condition.

For the oxidation of eutectic 63Sn-37Pb at 85°C in dry air in Fig. 4, the growth of SnO is similar in thickness to the pure Sn up to 4 days. However, under the T/H condition as shown in Fig. 5, SnO<sub>2</sub> grew excessively after 1 day while SnO remained almost the same amount ( $\sim 27$  Å) and no Pb oxide was found. The reduction potential of SnO in pure Sn and eutectic Sn-Pb was found to decrease with the oxidation time, suggesting that the Sn oxides may exist as a mixture of SnO and SnO<sub>2</sub>. This is consistent with the observation from the mixture of SnO and SnO<sub>2</sub> powders, where the reduction potential continuously decreases during the reduction of SnO.

In summary, the sequential electrochemical reduction analysis method (SERA) has been successfully applied to obtain the information on both the nature of oxide and oxide thicknesses created on pure Sn and eutectic 63Sn-37Pb solder under different oxidizing conditions. The SnO grows faster under a humid condition than in dry air at 85°C and a very thin SnO<sub>2</sub> overlayer was formed on the top surfaces of both alloys. For eutectic 63Sn-37Pb, Sn oxides form as a mixture layer of SnO and SnO<sub>2</sub>, and SnO<sub>2</sub> grows excessively for a prolonged time of up to 10 days under the humid condition at 85°C. Further investigation is in progress with other alloys such as Pb-rich and Pb-free solders to better understand their oxidation behaviors and mechanisms and thereby alleviate any reliability concerns associated with them.

## ACKNOWLEDGEMENT

This work was supported by the Center for Electronic Packaging Materials of Korea Science and Engineering Foundation. One of the authors, Sung-il Cho, received support from the Brain Korea 21 program. The authors wish to thank Dr. Donald W. Henderson for providing the SERA equipment and discussing the experimental results in the early stage of the investigation.

## REFERENCES

1. A. T. Fromhold, Jr., *Theory of Metal Oxidation, Vol. 1 Fundamentals*, North-Holland Publishing Company, 1976.
2. Marcel Pourbaix, *Atlas of Electrochemical Equilibria in Aqueous Solutions*. Pergamon Press, 1966.
3. Frederick G. Yost, F. Michael Hosking, and Darrel R. Frear, *The Mechanics of Solder Alloy, Wetting & Spreading*, Van Nostrand Reinhold, 1993.
4. D. Morgan Tench, D. P. Anderson, and P. Kim, *J. Appl. Electrochem.*, **24** (1994) 18.
5. Rao R. Tummala et al., *Fundamentals of Microsystems Packaging*, McGraw-Hill, 2001.
6. D. A. Sluzewski, Y. A. Chang, and V. C. Marcotte, *Mat. Res. Soc. Symp. Proc.* **167** (1990) 353.
7. E. E. de Kluizenaar, *J. Vac. Sci. Technol. A* **1(3)** (1983) 1480.
8. T. Farrell, *Met. Sci.*, **10** March (1976) 87.
9. A. J. Bevolo, J. D. Verhoeven, and M. Noack, *Surf. Sci.*, **134** (1983) 499.
10. M. L. Varsányi, J. Jaén, A. Vértes, and L. Kiss, *Electrochim. Acta*, **30(4)** (1985) 529.
11. S. N. Shah and D. Eurof Davies, *Electrochim. Acta*, **8** (1963) 663.
12. S. E. S. El Wakkad, A. M. Shams Dl Din, and Jeannette A. El Sayed, *J. Chem. Soc. Lond.*, (1954) 3103.
13. David R. Lide, *Handbook of Chemistry and Physics*, 73rd edition, CRC Press. 5-75
14. C. I. House and G. H. Kelsall, *Electrochim. Acta*, **29(10)** (1984) 1459.
15. Peter Bratin, Michael Pavlov, and Gene Chalyt, Research Report from Homepage of ECI technology ([www.ecitechnology.com](http://www.ecitechnology.com)).

Table 1. Reduction potentials of Pb and Sn oxides and Sn hydroxides.

| Oxide               | Free Energy of Formation <sup>11</sup> , $\Delta G^\circ$ (298K, kJ/mole) | Equilibrium potential (V) | Measured potential by SERA (V) |
|---------------------|---|---------------------------|--------------------------------|
| PbO                 | -187.9  | -0.4639                   | -0.554                         |
| SnO                 | -251.9  | -0.7955                   | -0.972                         |
| SnO <sub>2</sub>    | -515.8  | -0.8266                   | -1.10                          |
| Sn(OH) <sub>2</sub> | -491.6 <sup>12</sup>  | -0.8090                   |                                |
| Sn(OH) <sub>4</sub> | -952.5  | -0.7295                   |                                |

Fig. 1. Oxide reduction potentials measured for oxide powders by SERA.

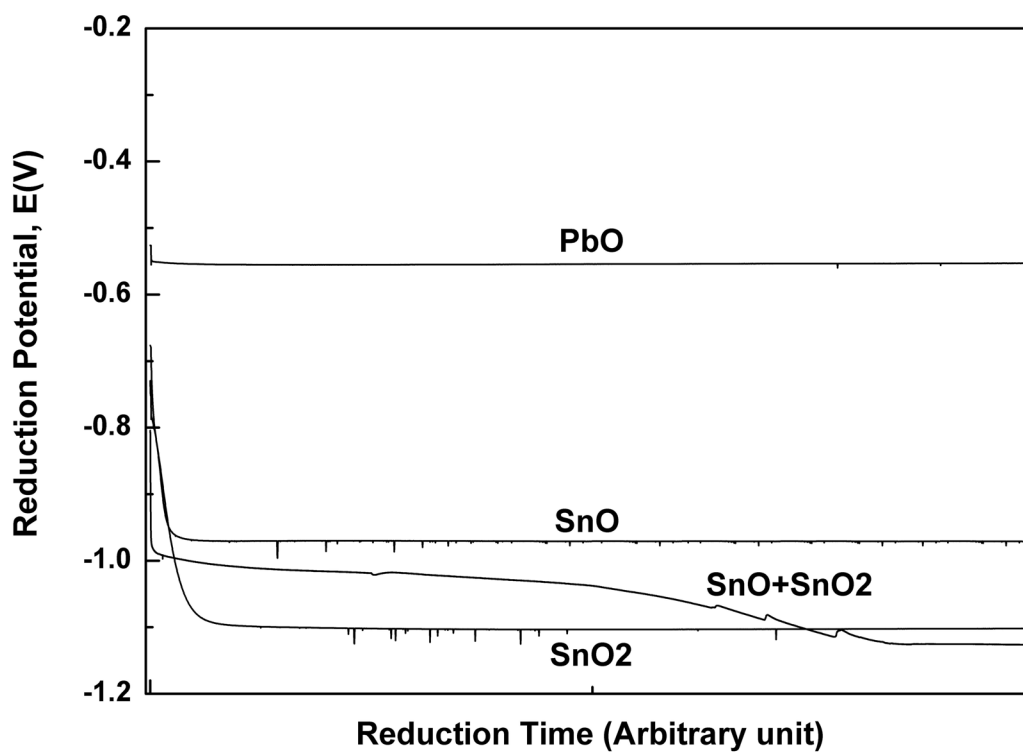


Fig. 2. SERA reduction curves for pure Sn oxidized at 85°C in dry air for several times.

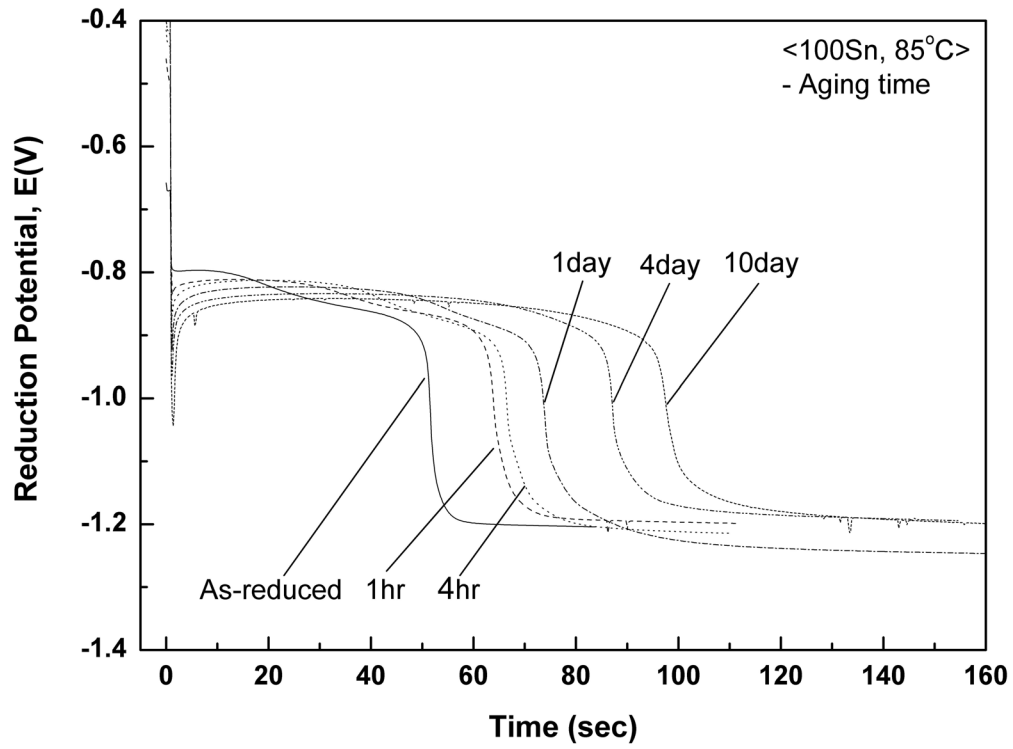


Fig. 3. SERA reduction curves for pure Sn oxidized at T/H for several times.

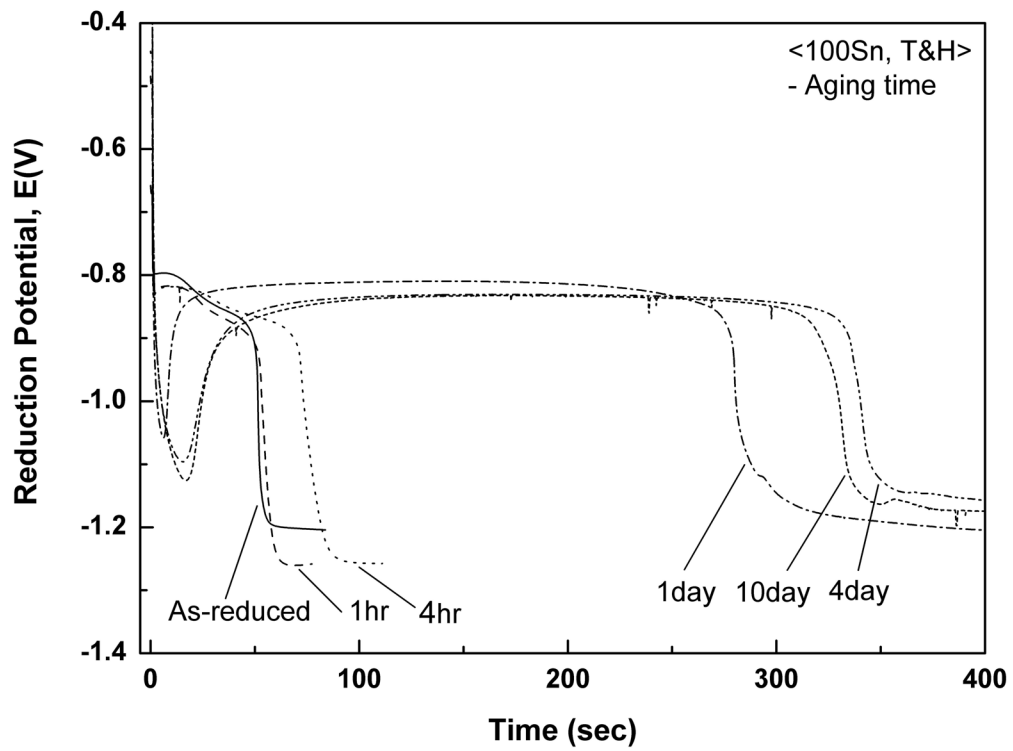




Fig. 4. SERA reduction curves for 63Sn-37Pb oxidized at 85°C in dry air for several times.

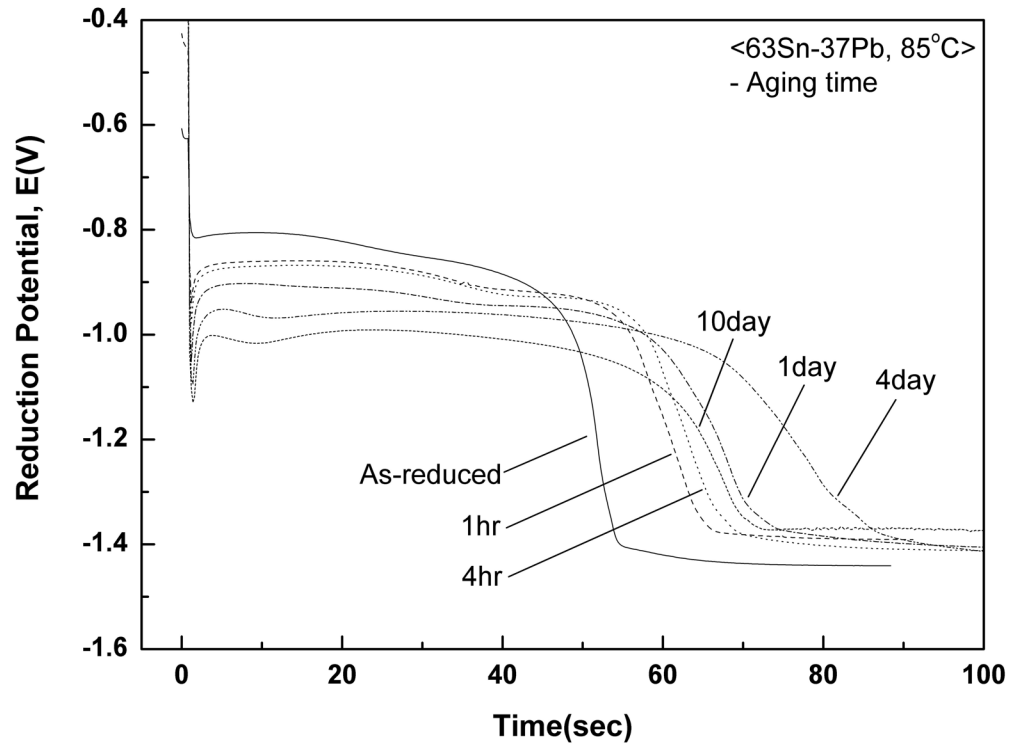


Fig. 5. SERA reduction curves for 63Sn-37Pb oxidized at T/H for several times.

